Available online at www.sciencedirect.com

ScienceDirect

Ceramics International 40 (2014) 4691–4696

CERAMICS INTERNATIONAL

www.elsevier.com/locate/ceramint

The optical properties and sunscreen application of spherical h-BN–TiO_2/mica composite powder

Cherng-Yuh Su[a,*], Hong-Zheng Tang[a], Geng-De Zhu[b], Chia-Ching Li[c], Chung-Kwei Lin[d]

[a]*Institute of Manufacturing Technology, National Taipei University of Technology, Taipei 106, Taiwan*
[b]*National Nitride Technologies Co. Ltd., Taichung 411, Taiwan*
[c]*Department of Cosmetic Science, Vanung University, Taoyuan 320, Taiwan*
[d]*School of Dental Technology, College of Oral Medicine, Taipei Medical University, Taipei 110, Taiwan*

Received 27 July 2013; received in revised form 3 September 2013; accepted 3 September 2013
Available online 13 September 2013

Abstract

In the present study, TiO_2/mica and hexagonal boron nitride powders were used as the starting materials to prepare composite powders by mechanical mixing and spray drying. The starting powders, as-prepared powders, and nano-TiO_2 were examined by scanning electron microscopy, particle-size analysis, and X-ray diffraction to reveal the powder morphology, particle size distribution, and crystalline phases. These powders were added to linseed oil to prepare emulsions for sunscreen applications. The powder-added emulsions were examined by UV–visible spectroscopy and a sun protection factor tester. The experimental results showed that the emulsion with spray-dried powder exhibited a significant improvement in sunscreen protection performance and was superior to its nano-TiO_2 counterpart.

Keywords: Titanium dioxide; Boron Nitride; C. Optical properties; SPF; Cosmetics

1. Introduction

The solar radiation reaching the surface of earth includes ultraviolet (200–400 nm), visible light (400–760 nm), and infrared region (760–4000 nm) [1]. The ultraviolet light is more detrimental to human body and can be classified into UVC (200–290 nm), UVB (290–320 nm), and UVA (320–400 nm) [2] The ultraviolet light within UVC is mostly blocked by the ozone layer in Earth's atmosphere surrounding the earth [3] UVB and UVA induce the main damage to the human skin. UVB, with shorter wavelength than UVA and higher energy, causes redness on epidermis of the skin and induce serious DNA damage [4]. Whereas UVA has less energy and causes weaker sunburn. The longer wavelength of UVA, however, can reach the dermis layer. Prolonged exposure under UVA can stimulate melanin and cause the degeneration of collagen and elastin on the dermis layer. Thus this may reduce the elasticity of skin resulting in wrinkles, and even lead to the occurrence of free radicals damaging the skin cells [5].

For sunscreen protection, cosmetics is the most commonly used material. The protection mechanisms of cosmetics are either chemical or physical. The chemical sunscreen agents use organic compounds to absorb UV light. Commercially available high sunscreen protection factor (i.e., SPF) products usually contain high concentration of organic compounds that may experience durability problem after prolonged UV radiation. This may induce either phototoxic or photochemical reactions and lead to skin irritation [6]. The physical sunscreen agents generally applies inorganic powder to absorb, reflect, and refract the ultraviolet light and has less irritation and allergic problems on skin. Many inorganic UV blocking materials, such as titanium dioxide, mica, boron nitride have been used successfully in cosmetic industry [7,8] . To improve further the sunscreen protection ability, modification of these materials have been attempted. For instances, it has been reported that nanocrystalline titania exhibited superior UV absorption ability than its conventional micron-size counterpart [9]. Jaroenworaluck et al. synthesized silica-coated TiO_2 nanoparticles that can be used for sunscreen application [10].

*Corresponding author. Tel.: +886 2 27712171x2044; fax: +886 2 27764889.
E-mail address: cysu@ntut.edu.tw (C.-Y. Su).

0272-8842/$ - see front matter © 2013 Elsevier Ltd and Techna Group S.r.l. All rights reserved.
http://dx.doi.org/10.1016/j.ceramint.2013.09.010

Ren et al. reported that the reflectance of TiO_2-coated mica increases with increasing amount of TiO_2 [11]. In addition, BN-coated CeO_2 particles exhibited higher transparency and more effective UV blocking performance than conventional TiO_2 or ZnO-coated CeO_2 particles [12].

In the present study, titanium dioxide coated mica (TiO_2/mica) and boron nitride powder were used as the starting materials. Mechanical mixing and spray drying processes will be used to prepare composite powders. The starting materials and as-prepared composite powders will be characterized by scanning electron microscopy, particle size analyzer, and X-ray diffraction. The emulsion will be prepared by adding the powders (starting material, composite powder, and prototype nano-TiO_2 powder) into linseed oil and the corresponding optical properties will be investigated.

2. Experimental

2.1. Preparation of TiO_2/mica and h-BN composite powders

In the present study, two commercially available powders were used as the starting materials that were composite-type TiO_2/mica (UV909, Sunshine Mineral Company Co., Ltd. Taitung, Taiwan) and h-BN (Cna04, National Nitride Technologies Co., Ltd. Taichung, Taiwan) powders. Two different types of processing, i.e., mechanical mixing and spray drying, were used to mix homogeneously these two starting powders and synthesize composite powders. For mechanical mixing process, TiO_2/mica (400 g) and h-BN (100 g) powder was mechanically mixed using an attritor mill under an ambient environment. Whereas for spray drying process, TiO_2/Mica (400 g) and h-BN powder (100 g) were added to D.I water (1000 ml), magnetically stirred and ball milled to obtain homogenous TiO_2/Mica and h-BN dispersed solution. Then the dispersed solution was fed into spray drying system (CNK SDDNO-3, IDTA Machinery Co., Ltd., Taipei, Taiwan) using the process parameters of: in air = 180–200 °C, out air = 70–90 °C, chamber = 80–100 °C, press air is ~1.5 kg/cm^2, and the feed rate is ~3 kg/hr. The as-prepared powder was then sintered at 800 °C for 1 hr. Detailed equipment setup is illustrated in Fig. 1.

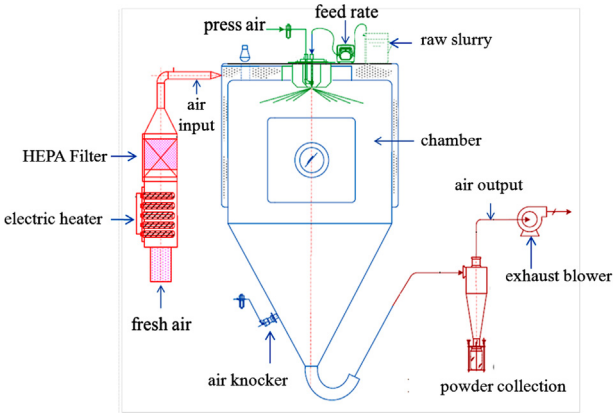

Fig. 1. Schematic illustration of spray drying system.

2.2. Characterization

The surface morphology was observed by an field emission scanning electron microscope (JSM-6500F, JEOL Co., Ltd., Japan) using secondary electron (SEI) method to observe powder surface morphology. The particle size analysis was examined by a particle size analyzer (SALD-201V, SHIMADZU Co., Ltd. Japan) using dynamic light scattering mode to measure the particle size distribution. Whereas an X-ray diffractometer (PW3040/60, X'pert PRO, PANalytical Co., Ltd., The Netherlands) was used to examine the crystalline structure of various powders.

For optical and sunscreen properties characterization, TiO_2/Mica, h-BN, TiO_2/mica + h-BN (mechanical mixing) and TiO_2/mica + h-BN (spray drying) powders were examined. In addition, commercially available nano-TiO_2 (TU-1125 R-type, Yong-Zhen Technomaterial Co., Ltd. Taipei Taiwan) was also evaluated for comparison. Each kind of powder was mixed with linseed oil according to a weight ratio of 1: 4. The optical characteristics were examined by UV–vis spectrophotometer (UV-3600 UV–vis-NIR Spectrophotometer, SHIMADZU Co., Ltd. Japan). The emulsion samples (powder mixed with linseed oil) were placed into a quartz plate with a $10 \times 10 \times 1$ mm^3, the UV–vis detection wavelength was ranged from 220–800 nm (i.e., UVC-IRA range). From the UV–vis spectrum, the absorption intensity, the characteristic peak, and red/blue phenomenon can be determined. A sun protection factor tester (SPF-290S, Optometrics Co., Ltd. USA) was used to determine the SPF value of each sample within a wavelength length ranged from 290 to 400 nm. The emulsion samples (2 mg/cm^2) were coated on a 3M transparent film and placed for ~20 min before SPF examination. The sun protection factor test was performed on 6 different locations on the film to determine the SPF value of each sample [13]. Critical wavelength [14] can also be obtained to explore the sun-effectiveness based on US-FDA proposed rule [15].

3. Results and discussion

3.1. Powder characterization

Fig. 2 shows the SEM images of various powders investigated in the present study. The TiO_2/mica starting powder had an average grain size of ~8.0 μm, as shown in Fig. 2(a), and the TiO_2/mica particle was plate-like. The high-magnification SEM image seen in Fig. 2(b) shows the surface of mica (i.e., the plate) uniformly coated by nanocrystalline TiO_2 powder. Another starting powder, hexagonal boron nitride (h-BN) was also plate-like, with an average grain size of ~2 μm, which was smaller than that of TiO_2/mica powder. Fig. 2(c) shows an SEM image of h-BN powder that looked similar to the image of TiO_2/mica powder shown in Fig. 2(a). After mechanical mixing of the TiO_2/mica and h-BN starting powders, the plate-like morphology was not altered significantly. The SEM image of the mechanically mixed powder, seen in Fig. 2(d), shows agglomeration of plate-like particles. The spray-dried powder particles, however, were spherical and different from those of

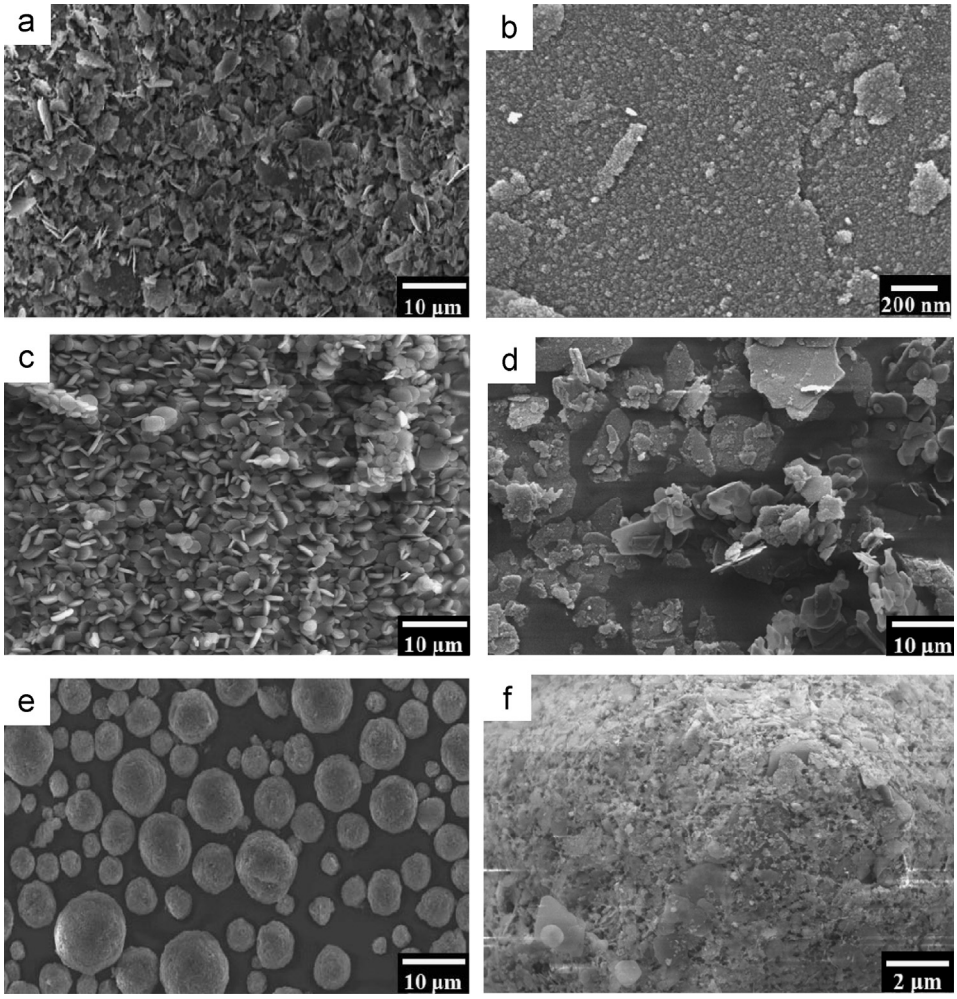

Fig. 2. SEM images showing the powder morphology of (a) TiO_2/mica, (b) TiO_2/mica (with higher magnification), (c) h-BN, (d) mechanically mixed TiO_2/mica and h-BN, (e) spray-dried TiO_2/mica and h-BN, and (f) spray-dried TiO_2/mica and h-BN (with higher magnification).

the starting powders, as shown in Fig. 2(e). A higher-magnification image of the spray-dried powder (Fig. 2(f)) shows that the spherical spray-dried powder consisted of large amounts of submicron granular particles and some plate-like particles (~2 μm).

A particle size analyzer was used to further examine the as-prepared composite powders, and Fig. 3 shows the corresponding results. The mechanically mixed TiO_2/mica and h-BN powder exhibited a bimodal distribution, where two modes can be seen in the particle size distribution shown in Fig. 3(a). The median size (D_{50}, representing 50% of the particles) of the particle size distribution was 8.8 μm. Fig. 3(b) shows that the particle-size distribution in the spray-dried composite powder was very close to a bell-shaped Gaussian distribution. The median size was 10.2 μm, slightly larger than that of the mechanically mixed powder.

Fig. 4 shows the X-ray diffraction patterns of the starting, mechanically mixed, and spray-dried composite powders. The TiO_2/mica powder, represented by curve (a), exhibited both mica and TiO_2 phases [16], while h-BN, represented by curve (b), showed a typical boron nitride phase [17,18], The mechanically mixed and spray-dried powders, represented by curves (c) and (d), respectively, exhibited the same phases as those of the starting powders. No extra phase could be found, indicating that neither mechanical mixing nor spray drying could induce phase transformation during the process.

In addition to the starting powders and as-prepared composite powders mentioned above, commercially available nanometer-sized TiO_2 powder (abbreviated as nano-TiO_2) was also used as a prototype for comparison. The corresponding SEM image and X-ray diffraction pattern are shown in Fig. 5(a) and (b), respectively, where nano-TiO_2 powder exhibited a grain size ranging from 10 to 20 nm and the rutile phase [19].

3.2. Optical properties and sunscreen characteristics

Five different powders—TiO_2/mica, h-BN, mechanically mixed TiO_2/mica and h-BN, spray-dried TiO_2/mica and h-BN, and nano-TiO_2 powders—were added to linseed oil to prepare individual emulsions for optical and sunscreen property examination. The optical property of each emulsion was first examined by UV–visible spectroscopy, and Fig. 6 shows the corresponding spectra of the five emulsions. The

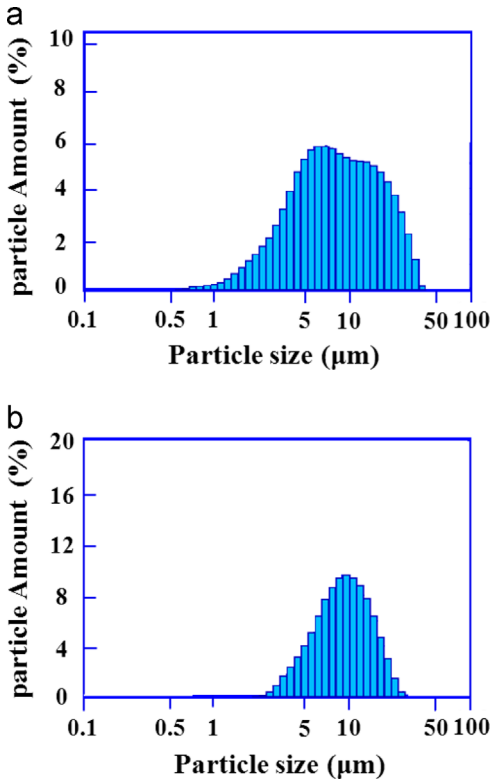

Fig. 3. Particle size distribution of (a) mechanically mixed (D_{50}=8.8 μm) and (b) spray-dried TiO_2/mica and h-BN powder (D_{50}=10.2 μm).

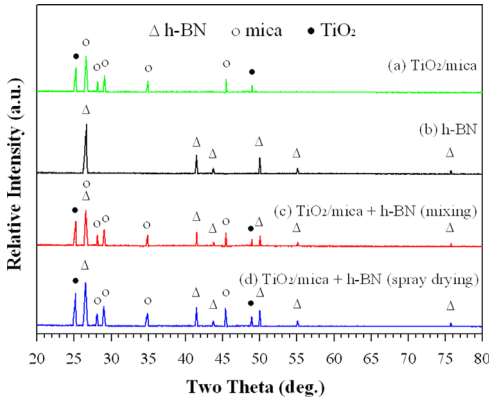

Fig. 4. X-ray diffraction patterns of (a) TiO_2/mica, (b) h-BN, (c) mechanically mixed TiO_2/mica and h-BN, and (d) spray-dried TiO_2/mica and h-BN.

UV–visible spectrum of the emulsion prepared from the spray-dried composite powder (Fig. 6(a)) exhibited a large absorption peak at a wavelength of ~260 nm. The respective spectra of the other four samples all showed a similar peak at ~250 nm. Monotonic decrease in absorption intensity with increasing wavelength was observed for all emulsions. In order to reveal the details of differences in the UV–visible spectra of the emulsions, each full spectrum was divided into two parts, i.e., UVC (220–290 nm) and UVB–UVA (290–400 nm) regions. Fig. 6(b) shows the UVC spectra in which the positions of the characteristic absorption peaks are marked. The emulsions prepared from the starting powders TiO_2/mica and h-BN exhibited a characteristic absorption peak at 252 and

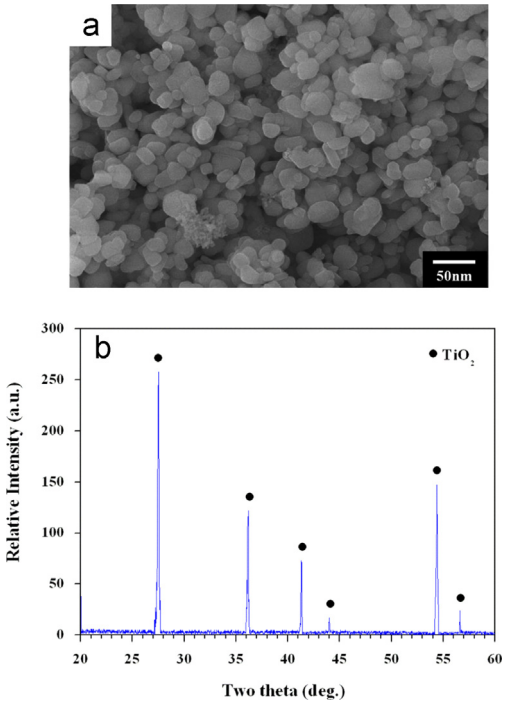

Fig. 5. (a) SEM image and (b) X-ray diffraction pattern of nano-TiO_2 powder.

254 nm, respectively, while that for the emulsion of mechanically mixed powder exhibited a peak at 250 nm. The emulsion prepared from nano-TiO_2 also showed a similar absorption peak at 254 nm. No significant difference between these peaks was observed. The emulsion with spray-dried composite powder, however, showed a red-shifted peak at 262 nm that was significantly larger than the peaks shown by other emulsions. Fig. 6(c) shows the absorption intensities within the UVB and UVA regions. It can be noted that within these regions, the spray-dried emulsion exhibited superior absorption performance when compared with the other four samples, whose absorption performances exhibited no significant differences within the UVB region. Meanwhile, the emulsion containing the mechanically mixed powder had slightly better performance than the emulsions containing the starting powders and nano-TiO_2 within the UVA region.

Su et al. simulated the effect of the particles' surface morphology on their light absorption. They suggested that light absorption increased with the number of reflections on a rough surface [20]. In the present study, the spray-dried powder containing spherical TiO_2/mica and h-BN exhibited a higher number of reflections compared to its plate-like, mechanically mixed (TiO_2/mica+h-BN) counterpart. In addition, the difference in surface morphology (i.e., spherical vs. plate-like) may induce different powder dispersion during the preparation of an emulsion [21]. Thus, the emulsion prepared from the spray-dried powder containing spherical TiO_2/mica and h-BN exhibited the best light absorption performance.

The sun protection factor, i.e., SPF, is another important metric in practical sunscreen protection. Table 1 summarizes the values of SPF and critical wavelength. The emulsions prepared from the starting powders, i.e., TiO_2/mica and h-BN,

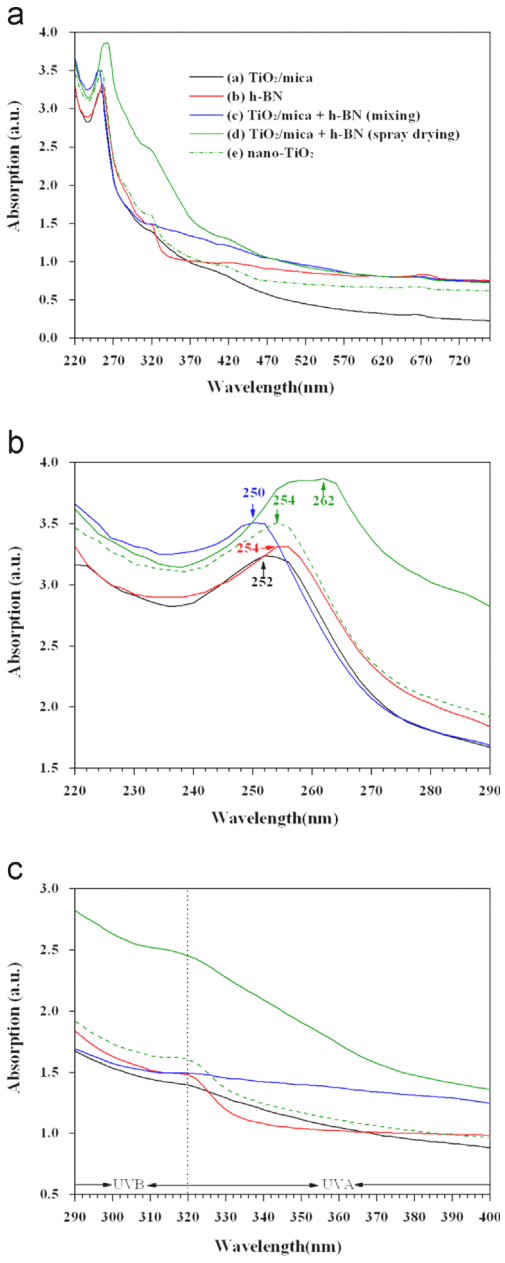

Fig. 6. (a) UVC–visible (220–760 nm), (b) UVC (220–290 nm), and (c) UVB–UVA (290–400 nm) absorption spectra of emulsions containing TiO_2/mica, h-BN, mechanically mixed TiO_2/mica and h-BN, spray-dried TiO_2/mica and h-BN, and nano-TiO_2.

Table 1
SPF and critical wavelength of TiO_2/Mica, h-BN, TiO_2/Mica+h-BN (mixing), TiO_2/Mica+h-BN (spray drying), and nano-TiO_2 added emulsion.

Material	US-FDA proposed rule	
SPF	Critical wavelength (nm)	
TiO_2/Mica	4.53	376.3
h-BN	3.75	372.5
TiO_2/Mica+h-BN (mixing)	4.91	381.1
TiO_2/Mica+h-BN (spray drying)	7.12	382.0
nano-TiO_2	7.03	378.5

exhibited SPF values of 4.53 and 3.75, respectively. The SPF value increased to 4.91 for the emulsion prepared from the mechanically mixed powder. A significant increase to 7.12, however, was observed for the emulsion of the spray-dried powder. This value was even slightly better than that of its nano-TiO_2 counterpart (7.03). In addition to the SPF values, the critical wavelengths (corresponding to 90% of the absorption within the 290–400 nm range of the spectrum) of these emulsions were also obtained from the measurements. It has been shown that the larger the critical wavelength, the better the sunscreen protection in the ultraviolet region [22]. The critical wavelengths of the TiO_2/mica and h-BN samples were 376.3 and 372.5 nm, respectively. They increased to ~380 nm for both mechanically mixed and spray-dried samples, which were superior to that of the nano-TiO_2 sample (378.5 nm).

4. Conclusions

In the present study, TiO_2/mica and h-BN powder were mechanically mixed and spray dried to synthesize composite powder. For mechanically mixed and spray dried powder, the median size of the particle size distribution is 8.8 and 10.2 μm, respectively. No phase transformation can be noticed during mechanical mixing and spray drying process. The TiO_2/mica, h-BN, and mechanically mixed TiO_2/mica and h-BN added emulsion show respectively a absorption peak at 252, 254, and 250 nm, similar to that with nano-TiO_2 (254 nm). A red shift to 262 nm, however, can be noticed for the emulsion with spray dried composite powder. The emulsion with spray dried composite powder, exhibits not only a significant improvement in sun protection factor but also an increase in critical wavelength. Both are superior than those of its nano-TiO_2 counterpart.

Acknowledgments

This work was supported by the National Taipei University of Technology-Taipei Medical University Joint Research Program, (NTUT-TMU-102-02).The authors thank Associate Professor S.M. Chang (National Taipei University of Technology, Institute of Organic and Polymeric Materials, Taipei, Taiwan) for their assistance with UV–vis-NIR Spectrophotometer measurements.

References

[1] P. Schroeder, J. Haendeler, J. Krutmann, The role of near infrared radiation in photoaging of the skin, Experimental Gerontology 43 (7) (2008) 629–632.
[2] P. Schroeder, C. Calles, T. Benesova, F. MacAluso, J. Krutmann, Photoprotection beyond ultraviolet radiation – effective sun protection has to include protection against infrared a radiation-induced skin damage, Skin Pharmacology and Physiology 23 (1) (2010) 15–17.
[3] B.L. Diffey, Human exposure to solar ultraviolet radiation, Journal of Cosmetic Dermatology 1 (3) (2002) 124–130.
[4] B.L. Diffey, Ultraviolet radiation and human health, Clinics in Dermatology 16 (1) (1998) 83–89.
[5] B.L. Diffey, What is light? Photodermatology Photoimmunology and Photomedicine 18 (2) (2002) 68–74.

[6] J.H. Epstein, Phototoxicity and photoallergy in man, Journal of the American Academy of Dermatology 8 (2) (1983) 141–147.
[7] M.I. Carretero, M. Pozo, Clay and non-clay minerals in the pharmaceutical and cosmetic industries part II active ingredients, Applied Clay Science 47 (3–4) (2010) 171–181.
[8] M. Engler, C. Lesniak, R. Damasch, B. Ruisinger, J. Eichler, Hexagonal boron nitride (hBN) – applications from metallurgy to cosmetics. [Hexagonales Bornitrid (hBN) – Anwendungen von Metallurgie bis Kosmetik], CFI Ceramic Forum International 84 (12) (2007) (D25-D29+E49-E53).
[9] C. Lin, W. Lin, Sun protection factor analysis of sunscreens containing titanium dioxide nanoparticles, Journal of Food and Drug Analysis 19 (1) (2011) 1–8.
[10] A. Jaroenworaluck, W. Sunsaneeyametha, N. Kosachan, R. Stevens, Characteristics of silica-coated TiO_2 and its UV absorption for sunscreen cosmetic applications, Surface and Interface Analysis 38 (4) (2006) 473–477.
[11] M. Ren, H. Yin, A. Wang, T. Jiang, Y. Wada, Mica coated by direct deposition of rutile TiO_2 nanoparticles and the optical properties, Materials Chemistry and Physics 103 (2–3) (2007) 230–234.
[12] T. Masui, M. Yamamoto, T. Sakata, H. Mori, G. Adachi, Synthesis of BN-coated CeO_2 fine powder as a new UV blocking material, Journal of Materials Chemistry 10 (2) (2000) 353–357.
[13] J.R. Villalobos-Hernández, C.C. Müller-Goymann, In vitro erythemal UV-A protection factors of inorganic sunscreens distributed in aqueous media using carnauba wax-decyl oleate nanoparticles, European Journal of Pharmaceutics and Biopharmaceutics 65 (1) (2007) 122–125.
[14] B.L.x Diffey, A method for broad spectrum classification of sunscreens, International Journal of Cosmetic Science 16 (2) (1994) 47–52.
[15] Sunscreen Drug Products for Over-the-Counter Human Use: Final Rules and Proposed Rules, Food and Drug Administration, (2011) 21 CFR Parts 201, 310, and 352.
[16] JCPDS Card No. 65-2448.
[17] JCPDS Card No. 34-0421.
[18] H. Tokoro, S. Fujii, T. Oku, T. Segi, S. Nasu, Materials Transactions 45 (9) (2004) 2941–2944.
[19] JCPDS Card No. 65-0191.
[20] F.G. Su, J.Q. Liang, Z.Z. Liang, W.B. Zhu, Acta Physica Sinica 60 (5) (2011) 057802.
[21] D.S. Schlossman, Method of coupling cosmetic materials and cosmetics containing coupled materials, United States Patent 5314683, 1994.
[22] B.L. Diffey, P.R. Tanner, P.J. Matts, J.F. Nash, In vitro assessment of the broad-spectrum ultraviolet protection of sunscreen products, Journal of the American Academy of Dermatology 43 (6) (2000) 1024–1035.